

See discussions, stats, and author profiles for this publication at: <https://www.researchgate.net/publication/229911961>

Synthesis and humidity sensitivity of conducting polyaniline in SBA-15

ARTICLE in JOURNAL OF APPLIED POLYMER SCIENCE · AUGUST 2004

Impact Factor: 1.77 · DOI: 10.1002/app.20586

CITATIONS

39

READS

12

6 AUTHORS, INCLUDING:



Nan Li

Jilin University

52 PUBLICATIONS 977 CITATIONS

SEE PROFILE



Wangchang Geng

Northwestern Polytechnical University

53 PUBLICATIONS 685 CITATIONS

SEE PROFILE



Tong Zhang

chemical

160 PUBLICATIONS 2,529 CITATIONS

SEE PROFILE



Shilun Qiu

Jilin University

259 PUBLICATIONS 7,894 CITATIONS

SEE PROFILE

Synthesis and Humidity Sensitivity of Conducting Polyaniline in SBA-15

Nan Li,¹ Xiaotian Li,² Wangchang Geng,² Tong Zhang,³ Yan Zuo,² Shilun Qiu¹

¹Department of Chemistry and State Key Laboratory of Inorganic Synthesis and Preparative Chemistry, Jilin University, Changchun, 130023, China

²Department of Material Science and Alan G. MacDiarmid Institute, Jilin University, 10 Qianwei Road, Changchun, 130012, China

³Department of Electronic Engineering, Jilin University, Changchun, 130023, China

Received 17 October 2003; accepted 29 February 2004

DOI 10.1002/app.20586

Published online in Wiley InterScience (www.interscience.wiley.com).

ABSTRACT: Conducting polyaniline (PANI) was synthesized in mesoporous silica SBA-15. The investigations of XRD, N₂ adsorption–desorption, and IR spectra confirm the existence of polyaniline in the channels of SBA-15 hosts. The impedance of PANI/SBA-15 composites was studied at different relative humidity (RH) levels, ranging from 11 to 95% RH. The loadings of PANI as well as the concentration of HCl solution have substantial influence on the impedance values. The variation in impedance value of all PANI/

SBA-15 composites is more obvious than that of bulk PANI samples at the same RH. All these results imply that PANI/SBA-15 composites may have better humidity-sensitive properties than those of bulk PANI samples. © 2004 Wiley Periodicals, Inc. *J Appl Polym Sci* 93: 1597–1601, 2004

Key words: conducting polymers; polyaniline; nanocomposites; humidity sensitivity; silicas

INTRODUCTION

Because of their attractive semiconducting properties conductive polymeric materials have recently been finding an increasing range of applications in the optoelectronic and microelectronic fields.^{1–6} Polyaniline is unique among the known conducting polymers because its conductivity is controlled by the doping levels of oxidation and protons. Scheme 1 shows the oxidation states of polyaniline (PANI), whose electric properties are sensitive to water, which provides a basis for potential application in sensors for humidity control. The unique feature of change in conductivity on exposure to an aqueous environment involves two main processes: adsorbed water molecules dissociate at imine nitrogen centers and a positive charge migrates through the polymer. Generally speaking, most of the imine units in bulk polyaniline are enveloped in the polymeric network, and only those on the surface have a chance of coming into contact with water, which affects its sensitivity to humidity. One approach to solve the problem is to synthesize polyaniline in low-dimension materials, such as membranes.^{7–13} Collins and Buckley¹⁴ demonstrated the chemical-sensing

properties of conductive polyaniline coated onto woven fabric material and found the polyaniline-coated fabric was more than 10 times as sensitive to humidity. Wu and Bein¹⁵ prepared a conducting filament of polyaniline in mesoporous silica MCM-41 and observed significant conductivity. With one-dimensional nanostructure and high specific surface area, materials like that may find application as humidity sensors.

In the present work, we synthesized polyaniline in mesoporous silica SBA-15 with a two-dimensional (2-D) hexagonal structure and investigated the properties of polyaniline from the perspective of applied science. The unique feature of polyaniline provides a basis for potential application as a sensor for humidity control.

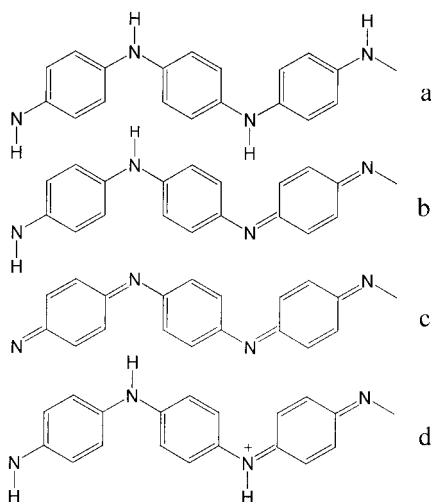
EXPERIMENTAL

Preparation of SBA-15

Silica SBA-15 was prepared according to processes and methods reported by Zhao et al.,¹⁶ using the triblock copolymer EO₂₀PO₇₀EO₂₀ (Pluronic P₁₂₃, Aldrich, Milwaukee, WI) and tetraethylorthosilicate (TEOS, 98%, Aldrich). The composition of the synthesis mixture was 0.8 g P₁₂₃, 25 mL H₂O, 4 mL HCl (37.5%), and 1.7 mL TEOS. After stirring at 313 K for 20 h, the mixture was crystallized at 373 K for 2 days. The SBA-15 products were collected by filtering and washed with distilled water. Subsequent heat treatment in air at 823 K removed the P₁₂₃ template.

Correspondence to: S. Qiu (sqiu@jlu.edu.cn).

Contract grant sponsor: National Natural Science Foundation of China; contract grant number: 20151001.



Scheme 1 Oxidation states of polyaniline: (a) leucoemeraldine; (b) emeraldine base; (c) pernigraniline; and (d) emeraldine salt.

Inclusion of PANI in SBA-15

The calcined SBA-15 was vacuumed to 10 Pa at 573 K for 24 h to remove air and water in the channels. Aniline was adsorbed into the pores of SBA-15 through vapor at various temperatures to obtain different loadings. The aniline-containing SBA-15 was immersed in the aqueous solution of $(\text{NH}_4)_2\text{S}_2\text{O}_8$ at 273 K under acid condition for 4 h. Finally, the products were washed with water and dried under vacuum. The preparation conditions and the polymer loading levels, calculated by means of thermogravimetric analysis (TGA), are shown in Table I.

Instruments

TGA was carried out on Perkin–Elmer TGA7 (Perkin Elmer Cetus Instruments, Norwalk, CT) in air at a heating rate of 20 K/min. The X-ray power diffraction patterns were obtained on a Siemens D-5005 diffractometer (Siemens AG, Karlsruhe, Germany) using Cu-K_α radiation at 40 kV and 35 mA. Diffractograms were recorded in the 2θ range 0.4 – 60° , at a scanning rate of 0.01° and a counting time of 1 s per step. Infrared spectra were taken on a Perkin–Elmer series

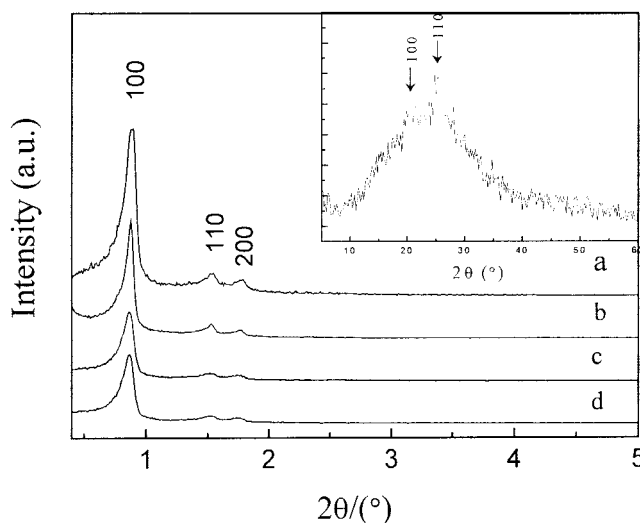


Figure 1 XRD patterns of (a) SBA-15, (b) PANI/SBA-15-1, (c) PANI/SBA-15-2, and (d) PANI/SBA-15-3. The inset shows the wide-angle XRD of the PANI/SBA-15-1 sample after the SBA-15 host was completely removed with HF solution.

with a resolution of 4 cm^{-1} . N_2 adsorption–desorption isotherms were measured at 77 K on a Micromeritics ASAP 2010m instrument (Micromeritics Instrument Corp., Norcross, GA). All samples were outgassed at 473 K for 20 h. The humidity dependency of the impedance spectroscopy was measured at room temperature for various relative humidity values on a ZL-5 model LCR analyzer at 1 kHz, room temperature, and 1.0 V (ac). A constant humidity environment was maintained by using aqueous solutions saturated with different salts: 11% (LiCl), 33% (MgCl_2), 54% [$\text{Mg}(\text{NO}_3)_2$], 75% (NaCl), 85% (KCl), and 95% (KNO_3). The PANI/SBA-15 powder materials were screen printed on a ceramic plate ($1 \times \frac{1}{2}$ in.) on which interdigitated gold electrodes were printed.

RESULTS AND DISCUSSION

X-ray diffraction

Power X-ray diffraction (XRD) patterns of SBA-15 and PANI/SBA-15 are shown in Figure 1. The existence of

TABLE I
Preparation Conditions and PANI Loading Levels for PANI/SBA-15 Samples

Sample	Temperature for aniline adsorption (K)	Concentration of HCl (mol/L)	$(\text{NH}_4)_2\text{S}_2\text{O}_8$ /aniline (mol/mol)	PANI loading (g/g SBA-15)
PANI/SBA-15-1	313	0.2	1	0.21
PANI/SBA-15-2	313	0.3	1	0.34
PANI/SBA-15-3	313	0.4	1	0.46
PANI/SBA-15-4	333	0.4	1	0.55
PANI/SBA-15-5	373	0.4	1	0.62

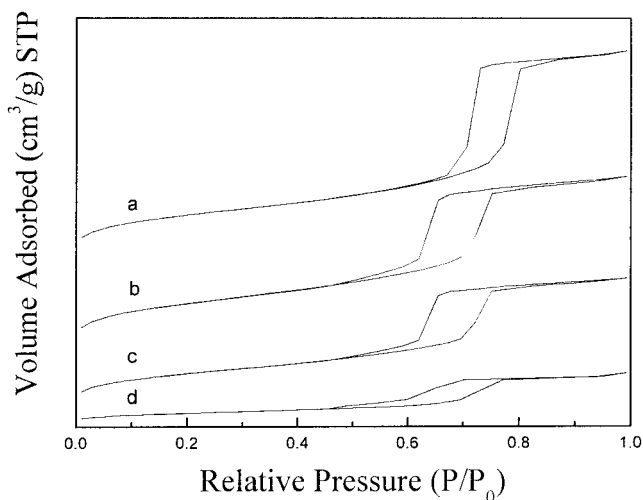


Figure 2 Nitrogen adsorption-desorption isotherms of (a) SBA-15, (b) PANI/SBA-15-1, (c) PANI/SBA-15-2, and (d) PANI/SBA-15-3.

three well-resolved peaks (d_{100} , d_{110} , d_{200}) suggests that the excellent hexagonal mesostructure of SBA-15 remained after inclusion of polyaniline.¹⁶ The intensity of peak (100) of SBA-15 substantially decreased with the increasing loading level of polyaniline because of the inclusion of polymer in the channel. The wide-angle XRD of the PANI/SBA-15 sample displays two reflections at $2\theta = 20.6^\circ$ (d_{100}) and $2\theta = 24.8^\circ$ (d_{110}), which are characteristic of polyaniline in emeraldine salt form.

N_2 adsorption-desorption isotherms

Figure 2 shows the N_2 adsorption-desorption isotherms for the parent SBA-15 and PANI/SBA-15. All isotherms are of type IV, respectively, suggesting the typical form of mesoporous materials. A well-defined step at the relative pressure $P/P_0 > 0.6$ can be observed for SBA-15. The isotherms for the PANI-containing samples are similar in shape to that of the parent SBA-15. As the loading of polyaniline increased, the amount of nitrogen absorbed decreases significantly, and the inflection point of step shifts to a smaller P/P_0 , which indicates that the inclusion of PANI into SBA-15 leads to a significant change in channel size. The difference of adsorption amount may be related to the change in channel shape in the SBA-15, which strongly influences the adsorption of N_2 on the sample.

IR spectroscopy

Infrared spectra of SBA-15 and PANI/SBA-15 are shown in Figures 3 and 4, respectively. The intense band at about 3435 cm^{-1} represents the Si—OH

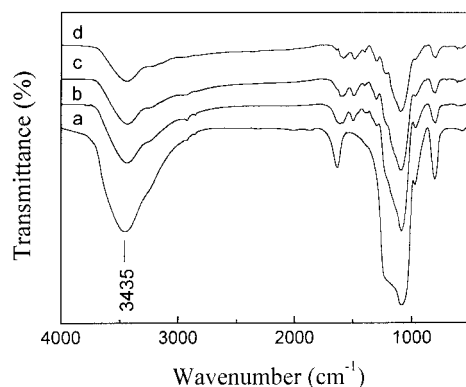


Figure 3 FTIR spectra of (a) SBA-15, (b) PANI/SBA-15-1, (c) PANI/SBA-15-2, and (d) PANI/SBA-15-3.

stretching vibration, which decreased with increasing loading amount. This suggests the intrachannel surface of SBA-15 is covered by polyaniline. The peak at 1640 cm^{-1} in FTIR observed in blank SBA-15 is attributed to the O—H bending vibration mode of the adsorbed water molecules. Encapsulation of polyaniline results in the formation of peaks at around 1600, 1500, and 1300 cm^{-1} , which are typical vibrations of emeraldine salt forms of polyaniline. Small shifts between IR frequencies of the polyaniline/SBA-15 composite and bulk PANI suggest some interaction of the polymer with the host.

Figure 5 shows the IR spectra of the PANI/SBA-15-1 sample taken before and after exposure to 33 and 75% RH. Adsorption of water from moist air results in enhancement of the peak at 3435 cm^{-1} . The peaks at 1505 and 1612 cm^{-1} can be assigned to C—N stretching from the benzenoid ring and quinone diimine radical, respectively. The intensity of the peak at 1612

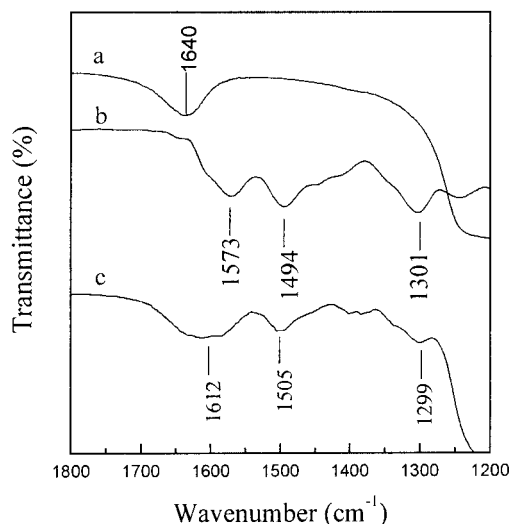


Figure 4 FTIR spectra of (a) SBA-15, (b) bulk polyaniline, and (c) PANI/SBA-15-1.

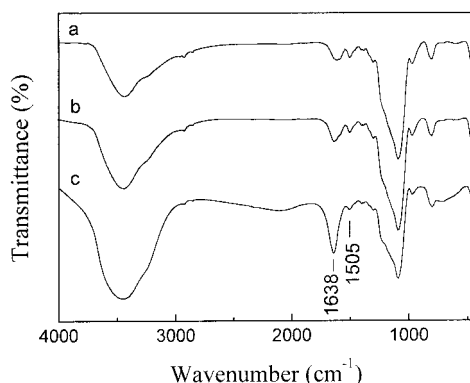
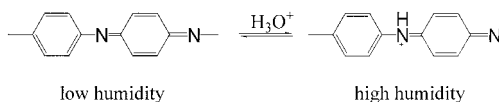


Figure 5 FTIR spectra of PANI/SBA-15-1: (a) as synthesized, (b) exposed to 33% RH, and (c) exposed to 75% RH.

cm^{-1} in the dry sample is comparable to that of the 1505 cm^{-1} peak. A slight increase in the peak intensity can be observed when the sample is subjected to 33% RH. On exposure to 75% RH, the peak becomes sharp and intense. The position of the peak shifts from 1612 to 1638 cm^{-1} . According to Matveeva¹⁷ and Ogura et al.,¹⁸ the reaction of polyaniline with residual water occurs as shown in Scheme 2. The amine nitrogen centers act as the acceptor of protons and the imine ones act as the donor of protons, which may account for the change of band at 1612 cm^{-1} under higher relative humidity.

Humidity sensitivity

Impedance of the PANI/SBA-15 composite is plotted versus the atmospheric humidity in Figure 6. Samples were placed in a sealed bottle in which a constant humidity environment was maintained. Impedance was recorded when it approached a constant value. Figure 6 shows the impedance of PANI/SBA-15 samples synthesized in various concentrations of HCl solution as a function of relative humidity. Impedance of the PANI/SBA-15-1 sample changed from $4.3 \times 10^3 \text{ k}\Omega$ to $1.8 \times 10^2 \text{ k}\Omega$ when the relative humidity increased from 11 to 95%. For samples PANI/SBA-15-2 and -3, the range is from 3.9×10^3 to $4.6 \times 10^2 \text{ k}\Omega$, and from 2.2×10^3 to $3.1 \times 10^1 \text{ k}\Omega$, respectively. The impedance for PANI/SBA-15-1 does not change significantly until the relative humidity increases to 54% RH because of the high resistance of the SBA-15 host. As expected, a decrease in the impedance at higher concentration of HCl can be observed, which is a



Scheme 2

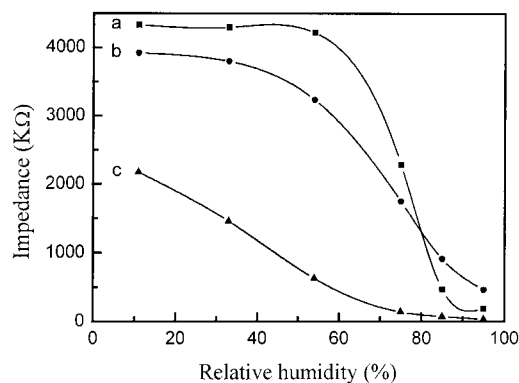


Figure 6 Impedance of PANI/SBA-15 synthesized in various concentrations of HCl solution as a function of relative humidity: (a) PANI/SBA-15-1, (b) PANI/SBA-15-2, and (c) PANI/SBA-15-3.

result of PANI proton doping and a specific configuration of a double bond between nitrogen and carbon atoms with a conjugation chain.^{3,17,19–23}

Impedance of PANI/SBA-15 with various PANI loadings as a function of relative humidity is shown in Figure 7. All samples are sensitive to humidity. The decrease in impedance of bulk polyaniline is limited to one order upon a change of relative humidity, which is comparable with literature results.^{18,24} The diagrams show that humidity sensing results in a modification by more than one order of magnitude of polymer impedance. For samples PANI/SBA-15-3, -4, and -5, the impedance changed from 2.1×10^3 to $3.1 \times 10^1 \text{ k}\Omega$, from 1.1×10^3 to $3.6 \times 10^1 \text{ k}\Omega$, and from 2.0×10^2 to $4.1 \text{ k}\Omega$, respectively. As the loading amount of PANI increases, the impedance at low humidity level (11% RH) significantly decreases. The impedance of sample PANI/SBA-15-5 is close to that of bulk PANI. The change in impedance is conspicuous at low relative humidity, and the linear portion extends from 11

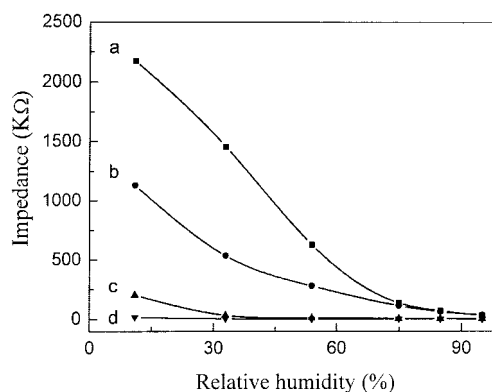


Figure 7 Impedance of PANI/SBA-15 with various PANI loadings as a function of relative humidity: (a) PANI/SBA-15-3, (b) PANI/SBA-15-4, (c) PANI/SBA-15-5, and (d) bulk PANI.

to 75% RH. At higher relative humidity, the impedance approaches a constant value. The range of the variation of the impedance for PANI/SBA-15 composites is notably higher than that of bulk polyaniline. Two reasons account for the changes in impedance: (1) Mesoporous silica SBA-15 is an insulator in the absence of water. With channels of 6–7 nm and Si—OH on the surface, SBA-15 easily adsorbs water from ambient air, which results in the decrease of resistance. (2) According to Scheme 2, water dissociates at the imine center ($\text{HOH} \leftrightarrow \text{H}^+ + \text{OH}^-$) and the proton incorporates into the polymer chain and π -conjugation of aromatic rings, which promotes easier electron transfer. This effect is comparable to that caused by acid doping of PANI. Moreover, in the composites of PANI/SBA-15, SBA-15 acts as a kind of substrate, in which PANI is dispersed on the surface of channels. Because of the small size of polyaniline in nanopores of SBA-15, the probabilities of the interaction between the imine units and the molecules of water in the PANI/SBA-15 composites are greater than that in bulk PANI.

CONCLUSIONS

The existence of polyaniline in the channels of SBA-15 was confirmed by XRD and N_2 adsorption–desorption. The peak at 1612 cm^{-1} , assigned to the vibration of quinone diimine radical cation in IR spectra, increased when the sample was exposed to 33 and 75% RH. This indicates the amine nitrogen centers act as an acceptor of protons. The impedance of PANI/SBA-15 composites was found to be sensitive to humidity. An increase in concentration of HCl solution as well as the amount of PANI loadings resulted in a decrease of impedance. The range of the variation of the impedance for PANI/SBA-15 composites is notably higher than that of bulk polyaniline.

The work was supported by National Natural Science Foundation of China (Grant 20151001).

References

1. Dogan, S.; Akbulcin, U.; Suzer, S.; Toppare, L. *Synth Met* 1993, 60, 27.
2. Kabayashi, T.; Yoneyama, H.; Tamura, H. *J Electroanal Chem* 1984, 161, 419.
3. Paul, E. W.; Ricco, A. J.; Wrighton, M. S. *J Phys Chem* 1985, 89, 1441.
4. Cao, Y.; Treacy, G. M.; Smith, P.; Heeger, A. J. *Appl Phys Lett* 1992, 60, 2711.
5. Parkhutik, V.; Martinez-Duart, J.; Diaz Calleja, R.; Matveeva, E. S. *J Electrochem Soc* 1993, 140, L94.
6. Matveeva, E.; Parkhutik, V.; Diaz Calleja, R.; Martinez-Duart, J. *J Lumin* 1993, 57, 175.
7. Riede, A.; Helmstedt, M.; Riede, V.; Zemek, J.; Stejskal, J. *Langmuir* 2000, 16, 6240.
8. Baba, A.; Advincula, R. C.; Knoll, W. *J Phys Chem B* 2002, 106, 1581.
9. Lee, Y. M.; Ha, S. Y.; Lee, Y. K.; Suh, D. H.; Hong, S. Y. *Ind Eng Chem Res* 1999, 38, 1917.
10. Han, C.-C.; Hong, S.-P. *Macromolecules* 2001, 34, 4937.
11. Tan, S.; Laforgue, A. D. *Langmuir* 2003, 19, 744.
12. Riede, A.; Helmstedt, M.; Riede, V.; Zemek, J.; Stejskal, J. *Langmuir* 2000, 16, 6240.
13. Kang, E. T.; Ma, Z. H.; Tan, K. L.; Tretinnikov, O. N.; Uyama, Y.; Ikada, Y. *Langmuir* 1999, 15, 5389.
14. Collins, G. E.; Buckley, L. J. *Synth Met* 1996, 78, 93.
15. Wu, C.; Bein, T. *Science* 1994, 264, 1757.
16. (a) Zhao, D.; Feng, J.; Huo, Q.; Melosh, N.; Fredrickson, G. H.; Chmelka, B. F.; Stucky, G. D. *Science* 1998, 279, 548; (b) Zhao, D.; Huo, Q.; Feng, J.; Chmelka, B. F.; Stucky, G. D. *J Am Chem Soc* 1998, 120, 6024.
17. Matveeva, E. S. *Synth Met* 1996, 79, 127.
18. Ogura, K.; Saino, T.; Nakayama, M.; Shiigi, H. *J Mater Chem* 1997, 7, 2363.
19. Angelopoulos, M.; Ray, A.; MacDiarmid, A. G.; Epstein, A. J. *Synth Met* 1987, 21, 21.
20. Epstein, A. J.; MacDiarmid, A. G. *Makromol Chem Macromol Symp* 1991, 51, 217.
21. Nechtschein, M.; Genoud, F.; Menardo, C.; Mizoguchi, K.; Travers, J. P.; Villeret, B. *Synth Met* 1989, 29, 211.
22. Ray, A.; Richter, A. F.; MacDiarmid, A. G.; Epstein, A. J. *Synth Met* 1989, 29, 151.
23. Rudzinski, W. E.; Lozano, L.; Walker, M. *J Electrochem Soc* 1990, 137, 3132.
24. Krutovertsev, S. A.; Ivanova, O. M.; Sorokin, S. I. *J Anal Chem* 2001, 56, 1057.